REVISION OF ACCELERATING AND DAMPING STRUCTURES FOR KEK STF 45 MV/m ACCELERATOR MODULES

Y. Morozumi*, F. Furuta, T. Higo, T. Saeki, K. Saito, KEK, 1-1 Oho, Tsukuba, 305-0801, Japan

Abstract

KEK is constructing its superconducting RF test facility and installing 1.3 GHz superconducting accelerator structures. Learning from experience with our first 45 MV/m 9-cell accelerating structures, we have redesigned the structures to improve the characteristics and the performances. Problems found in the earlier structures are resolved in the new structures.

INTRODUCTION

High Gradient Efforts

Accepting the final decision to choose superconducting radiofrequency (SRF) acceleration technology for the future linear collider in 2004, KEK terminated its own 11.4 GHz X-band linear collider (called GLC or JLC) project and joined the SRF-based 1.3 GHz L-band International Linear Collider (ILC) project. Ever since we have continued efforts to pursue the ultimate available accelerating gradient toward 51 MV/m [1, 2, 3, 4, 5]. Our high gradient activities are based on the idea that the fundamental limitation of gradient is given by thermal breakdown of superconductivity at the critical surface magnetic field and hence a higher gradient is achievable with a cavity geometry giving a higher field ratio H_{sp}/E_{acc} of the peak surface magnetic field H_{sp} to the accelerating gradient E_{acc} [6, 7]. Actually we have demonstrated high gradients over 50 MV/m up to 53.5 MV/m in single-cell cavities with a ratio H_{sp}/E_{acc} of 35.5 Oe/(MV/m) [2, 3, 4], which shows that the critical field is as high as 1900 Oe and that our symbolic target gradient of 51 MV/m is reachable in our 9-cell structures where a ratio H_{sp}/E_{acc} is about 37 Oe/(MV/m).

Superconducting RF Test Facility

In order to develop SRF technology and to establish a viable SRF accelerator design toward ILC, we have been constructing a SRF test facility (STF) [8], taking over the evacuated building which used to be occupied by an on-site J-PARC test linac. The original STF plan schedules the construction of two linacs on the underground floor in two phases. The 1st-phase linac consists of two half-span cryogenic accelerator modules (called cryomodules) housing four 45 MV/m 9-cell structures as well as four 35 MV/m 9-cell structures respectively and accelerating electrons from a DC gun to 270 MeV. The 2nd-phase linac comprises 3 full-span modules each accommodating eight 9-cell structures and accelerates electrons from an RF gun to 700 MeV. The facility includes an electro-polishing shop and a high pressure rinsing booth as well as a clean room and an assembly hall on the ground floor.

---

*moro@post.kek.jp

OLD DESIGN AND ITS PROBLEMS

Old Structures

The first design was based on an optimistic prospect that we would be able to soon realize the nominal gradient of 45 MV/m in 4 individual 9-cell structures and to remodel them into 2 pairs of so-called superstructures [9], each composed of twin 9-cell structures. The 9-cell structure has asymmetric end ports, one of which is a normal beam port, 80 mm in diameter while the other is a special port, 108 mm in diameter, to serve as an interconnect allowing two 9-cell structures to couple to each other when combined into a superstructure. The 108 mm port is terminated with a taper to 80 mm for convenience of connection to a normal beam pipe.

The damper design was borrowed from TESLA [10] in order to save time for a quick start of the high gradient program with four 9-cell structures.

One of the four structures was a plain structure without any couplers. The other three were equipped with dampers and a feeder port.
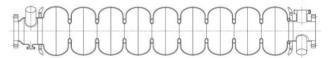

Figure 1: Sectional view of the old 9-cell structure. The left end port is a special one for the superstructure interconnection while the right end port is a regular one.

Limited Gradient Performance

As shown by excitation characteristics in Figure 2, the plain structure barely reached nearly 30 MV/m while the equipped structure fell short of 20 MV/m. Unlike single-cell cavities, these 9-cell structures have not been very successful in gradient performance. Multipacting (MP) was observed at over 7 MV/m in both the structures. In addition to multipacting, field emission (FE) also started around 15 MV/m showing a characteristic slope on the excitation curve in the equipped structure.
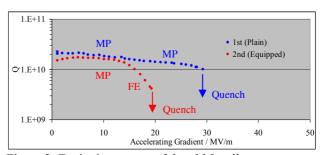

Figure 2: Excitation curves of the old 9-cell structures.

Multipacting and Field Emission in End Structure

The limitation of gradient in the plain structure was due to multipacting at the taper section of the end port. Figure 3 illustrates a typical trajectory of a possible tough multipacting around 28 MV/m. Energy analysis explains high secondary emission coefficientmat mean kinetic energy around 500 eV.
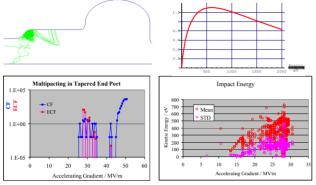

Figure 3: Multipacting at the end pot taper. a) Trajectory b) Counter and enhanced counter function c) assumed secondary emission coefficient d) energy statistics.

The gradient in the equipped structure was limited to 20 MV/m by field emission. Apparently the dampers were responsible since the plain structure did not suffer it.

We suspect that cavity surfaces are polluted with contaminated rinsing water and not only gain secondary emission yield to enhance multipacting, but also induce field emission. Ultra-pure water, for high-pressure rinsing after electro-polishing, tends to get polluted with contaminants from the pressure pump while it runs for more than 2 hours.

Leakage of Accelerating Mode Power

The damper with a built-in notch filter was supposed to decouple from the accelerating mode. Coupling was, however, not reduced without degrading higher order mode damping probably because the notch width was not wide enough to provide sufficient tunability. As a result we have to live with a compromise of insufficient decoupling from the accelerating mode and insufficient damping of higher order modes.

NEW DESIGN AND ITS FEATURES

New Structures

The new design is a total revision of the entire structure including dampers to facilitate the realization of an unattained gradient of or over 50 MV/m on which we set the top priority postponing the superstructure program. The special end structure for superstructure connection was replaced with an identical normal end structure to that on the other side. This modification leads to a slight improvement in accelerating structure performance.

The damping structure was also changed to suppress multipacting, to improve damping and decoupling

performance, and to simplify structures. Newly designed dampers were mounted in new positions and at new angles.

Figure 4: Sectional view of the new 9-cell structure. Both end ports are identical to the regular end port of the old 9-cell structure.

The structure parameters are tabulated below in comparison with those of the old design and of the TESLA design.

Table 1: Structure parameters. New design gains R/Q and improves the field ratios of Esp/Eacc and Hsp/Eacc.

	New	Old	TESLA
Aperture Diameter / mm	60	60	70
End Port Diameter / mm	80	80 / 108	78
Regular Cell Diameter / mm	98.151	98.151	103.3
Coupling Coefficient	0.0155	0.0155	0.0187
Geometric Impedance (R/Q) / Ω	1170	1144	1036
Geometric Factor	284	286	271
Esp/Eacc	2.36	2.38	2.0
Hsp/Eacc / Oe/(MV/m)	36.6	37.5	42.6
Max Eacc (Hc=1900 Oe) / MV/m	51.8	50.7	43.4

Suppression of Multipacting in End Structure

Multipacting in the end ports is eliminated since the tapered port has been replaced with a straight port where no multipacting is detected by simulation.

The new damper has an on-center main stem to keep distant from the wall for reduction in multipacting between the stem and the wall. The simple oval loop was introduced for ease of fabrication.
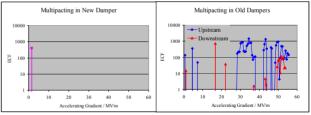

Figure 4: Multipacting in the new and the old dampers

Improvement in Higher Order Mode Damping

The loop orientation was chosen to give maximum coupling to HOM's and minimum coupling to the accelerating mode. The angular dependence of coupling is shown in Figure 4. Two dampers are mounted horizontally on one side and vertically on the other side since no clear evidence was seen for any preferred mounting angles.

Realistic damping effect was evaluated in simulation with a fine element model of a 9-cell structure with dampers.

External Q factor was computed for the accelerating mode (A), the 1st dipole modes (D1), the 2nd dipole

modes (D2) and the 3rd dipole modes (D3) varying the orientation angle from the beam axis. The maximum for the accelerating mode and the minimum for the dipole modes are simultaneously given at 180 degrees.
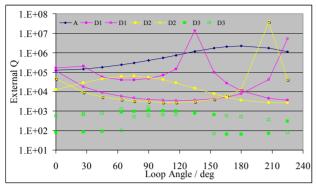

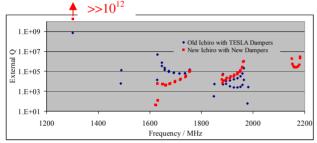Figure 5: Angular dependence of damper loop coupling.

Figure6: Damping performance in new and old structures.

Decoupling from Accelerating Mode

The external Q factor introduced by dampers is set at 10^{12} or above for the accelerating mode, more than 100 times as large as the intrinsic wall Q factor, so as to keep leakage power under 1% of the wall loss power.
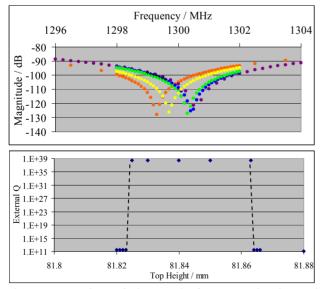

Figure 7: Tuning of the notch frequency in the end structure (a) and in the 9-cell structure (b).

In simulation with an end structure model the notch frequency is detected by a dip on transmission signal from the end cell to the damper. Figure 7a shows tuning by

adjustment of the top height of the damper. The sensitivity was 78 MHz/mm. In a 9-cell structure model a dip signal was hard to detect in or near the fundamental mode pass band and the external Q was directly computed for varied top height instead (Figure 7b). The notch width was estimated at 3 MHz for external Q higher than 10^{12}. The notch filter properly tuned at room temperature should stay tuned during cooling down to 2 K since thermal detuning is at most sub MHz. The new dampers will provide sufficient decoupling from the accelerating mode and sufficient damping of higher order modes as well.

PLAN AND PROSPECT

Damping of Higher-Frequency Modes

The damping effect on higher frequency modes than the cut-off is not straightforwardly evaluated either in simulation or in measurement since they propagate through beam ducts and interact with next 9-cell structures. Simple models of a 9-cell structure with truncated end ports do not give the right pictures either experimentally or computationally. Realistic simulation of damping higher-frequency higher-order modes is in preparation.

Realization of High Gradient

Although surface cleansing is essential to achieve high gradients, we are unfortunately suffering serious pollution of ultra-pure water for high pressure rinsing and we are suspending gradient test of the new 9-cell structures in the vertical cryostat. We have found the water pump is the source of contaminations. An alternative rinsing system is under examination. We are approaching slowly but steadily high gradients in 9-cell structures.

ACKNOWLEDGEMENTS

REFERENCES

[1] Sekutovicz et al, Proc. 20th Part. Acc. Conf. (PAC2005), Knoxville, June 2005, p.3342

[2] F. Furuta et al, Proc. 10th Eur. Part. Acc. Conf. (EPAC2006), Edingburgh, June 2006 p.750

[3] T. Saeki et al, Proc. 10th Eur. Part. Acc. Conf. (EPAC2006), Edingburgh, June 2006, p.756

[4] F. Furuta et al, Proc. 13th Int. Lin. Acc. Conf. (LINAC2006), Knoxville, August 2006, p.299

[5] T. Saeki et al, Proc. 13th Int. Lin. Acc. Conf. (LINAC2006), Knoxville, August 2006, p. 794

[6] K. Saito, Proc. 10th Int. Workshop on RF Superconductivity, Tsukuba, September 2001, p.583

[7] K. Saito, Proc. 11th Int. Workshop on RF Superconductivity, Lubeck, September 2003, MoO02

[8] H. Hayano et al, Proc. 31st Linac Technology Meeting (LAM31), Sendai, August 2006, FO23

[9] Sekutowicz et al, Phys. Rev. ST-AB2 (1999) 062001

07 Accelerator Technology Main Systems

T07 Superconducting RF